Instability of Steady Valve Flow in a Swirl Port

S.Tanabe, H.Iwata and Y.Kashiwada

Department of Mechanical Engineering
Tottori University
Kayama-cho
Tottori 630
Japan

ABSTRACT

Swirl generating characteristics of inlet port have been investigated for helical type of port from a production DI diesel engine by analyzing experimentally measured steady flow velocity distribution at the inlet valve curtain area, and unsteadiness of the velocity and its direction of the flow also has been investigated by measuring double components of the velocity at a coincident period.

INTRODUCTION

Velocity distribution and its fluctuation of inlet valve exit flow are valuable information in an port design for combustion improvement and an numerical simulation of in-cylinder gas motion. The helical port as a tool enhancing swirl producing capacity, in general, has both characteristics of spiral shaped port and directed port. The former produces pre-valve angular momentum flux around the valve axis and the latter post-valve component around the cylinder axis[1,2]. The helical port provides a higher swirl at lower and medium valve lift[3] and tends to produce more ordered motion in cylinder during compression and higher swirl inside bowl[4].

As for validity of quasi-steady flow assumption, laser anemometry measurements at the valve exit plane under steady and engine operating conditions have shown that good agreement is obtained during most of the valve opening period although there are differences during early and late induction [5,6]. At a fixed valve lift normalized velocity profiles are independent of flow rate[7].

Numerical simulations of evolution of in-cylinder swirl distribution during inlet and compression has been made[8,9], whereas input boundary conditions were given or determined by LDA at various valve lifts and circumferential locations under steady flow conditions and the in-cylinder flow was calculated at successive crank angles.

The valve flow velocity changes widely from time to time even in a steady flow condition, which unsteadiness gives rise to instability of swirl motion. In most cases, however, only time mean characteristics of the valve flow have been discussed. In this study flow characteristics of the helical port, including statistical analyses and angular momentum contribution to swirl generation, have been investigated by measuring three time-mean and instantaneous velocity components at the inlet valve curtain area under steady flow condition with two-dimension LDA system comprising the coincident data acquisition unit.

EXPERIMENTAL SYSTEM

Flow Configuration

Figure 1(a) shows the schematic diagram of an inlet port having a ramp helical type from a production DI diesel engine (bore x stroke: 100x110mm). The locations of velocity measurements are 1mm out of the valve curtain area, which is the annular opening between the valve head and seat, indicated by the letters
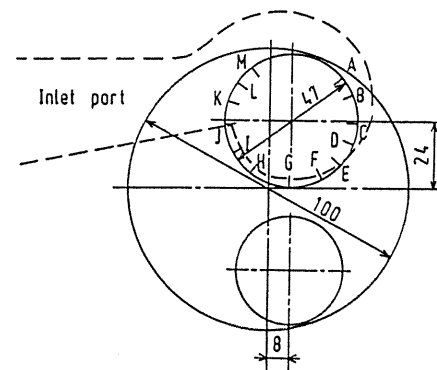

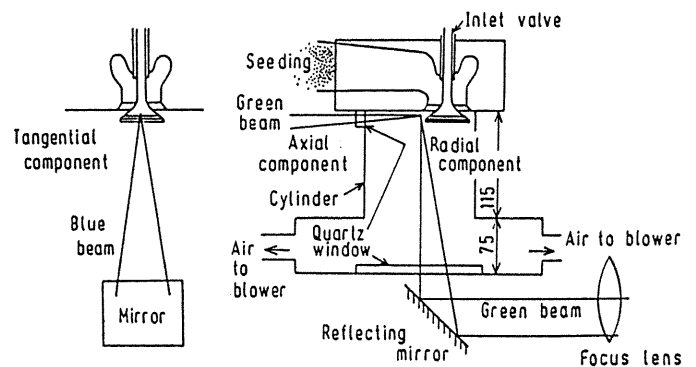Fig.1(a) Schematic diagram of cylinder head

Fig.1(b) Steady flow system and LDA arrangement for measuring the three components of velocity at valve curtain area

A,B,C····M and results were obtained at different distances from the cylinder head and different valve lifts. Figure 1(b) shows the steady flow system and LDA arrangement for measuring the three components of velocity at the valve curtain area. Air is induced through the port at a constant flow rate by a blower. After flowing through the cylinder, the air is distributed radially by eight pipes fixed at the air chamber on which the cylinder is mounted. On the bottom of chamber the quartz window of $\phi130$mm is installed for a laser beam acquisition. The cylinder diameter of $\phi100$mm is identical to that of the engine. The flow conditions are shown in Table 1.

Table 1

Valve lift (mm)	10	6
Location of velocity measurement from cylinder head (mm)	3,5,8	2,4
Air flow rate ($\times10^{-3}$ m^{-3}/s)	27.0	23.2
Mean cylinder column velocity (m/s)	3.44	2.95
Pressure difference between the port (Pa)	1510	1649

LDA System

Two-dimensional and two-color LDA system comprised 1.5W Argon-ion laser, transmitting optical units incorporating a Bragg cell with frequency shift of 40MHz and receiving units of a back scatter mode. As Fig.1(b) shows, two pairs of green and blue laser beams are compelled to bend by a right angle on a reflecting mirror, thus their incidence and fringe directions parallel the valve stem axis. The radial and tangential velocity components were measured by the green and blue one-D LDAs, respectively. Both velocity components were measured simultaneously by a coincidence unit which gave rise to data only when two effective doppler signals from the green and blue beams were simultaneously detected within a given short period of time, say 5μs. Crossing angles of the green and blue beams were about eight and sixteen degrees and their measurement volumes were $\phi0.107\times2.8$mm and $\phi0.104\times0.9$mm, respectively. These dimensions were determined using a $\phi5\mu$m tungsten wire running across the measurement volumes and based on e^{-2} doppler burst signal. Two measurement volumes formed at the beam crossings were adjusted definitely to come to a fixed point and the data were accessed with the coincidence unit, therefore, a resolvable distance of measurement was below 0.9mm toward the cylinder axial direction. The velocity measurement in the vicinity of the cylinder was impossible because of the beams interrupted by the cylinder.

The axial velocity component was measured by one-D LDA of green beam which was horizontally incident upon the quartz window of 15$\times$14mm and its measurement was carried out in separate hours from the other two velocity components.

The flow was seeded with atomized silicone oil droplets of 2μm mean diameter which were introduced through the upstream end of the port. The signal processing system was a high frequency counter which was interfaced to a microcomputer for data acquisition and proc-

essing. One thousand data were sampled at each measurement location. A counting number of burst signals was eight for frequency validity.

ANALYSIS OF THE FLOW

Figure 2 shows a schematic diagram in plane view of an offset inlet valve geometry, indicating the projection of the local velocity vector onto the plane perpendicular to the valve axis and comprising a tangential Vϕ and a radial Vr velocity components. The inlet angular momentum flux Hin with respect to the cylinder axis is given by the following equation(2),

$$Hin = \rho\ Rv \int_0^{2\pi}\int_0^L VrV\phi(Rv - e\cos\Phi)\ d\Phi\ dX$$
$$+\ \rho\ Rv \int_0^{2\pi}\int_0^L Vr^2\ e\ \sin\Phi\ d\Phi\ dX \qquad (1)$$

where L is valve lift, Rv is valve radius, e is valve eccentricity, Φ is azimuthal angle, X is axial distance from cylinder head and ρ is air density. The first and second terms of the right hand side of Eq.1 represent, respectively, the contributions of the tangential and radial velocity components to the inlet angular momentum flux, being expressed by Hϕ and Hr, respectively. The latter flux, in particular, represents the contribution of the port's orientation to the generated total angular momentum. The terms (Rv-ecosΦ) and e sinΦ represent, respectively, the arm lengths of the tangential and radial components from the cylinder axis. The contribution of the velocity component Vϕ in Eq.1 can be further divided into two parts

$$H\phi = \rho\ Rv^2 \int_0^{2\pi}\int_0^L VrV\phi\ d\Phi\ dX$$

$$-\ \rho\ Rv\ e \int_0^{2\pi}\int_0^L VrV\phi\cos\Phi\ d\Phi\ dX \qquad (2)$$

The first part of Eq.2 represents the inflow of angular momentum Hϕ1 with respect to the valve axis, previously referred to as pre -valve swirl component. The second one does the angular momentum inflow Hϕ2 with respect to the cylinder axis due to the Vϕ velocity component and the eccentricity of the valve, referred to as post-valve swirl. If Hϕ in Eq.1 is replaced by Eq.2, the following expression
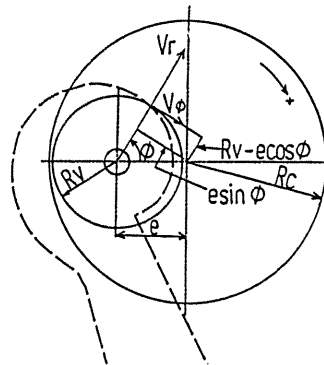

Fig.2 Schematic diagram of offset inlet valve geometry and notation for the analysis

for the total angular momentum flux Hin is obtained

$$Hin = H\phi1 + H\phi2 + Hr \qquad (3)$$

where

Hϕ1 :angular momentum w.r.t. the valve axis due to Vϕ velocity component (pre-valve swirl)

Hϕ2 :angular momentum w.r.t. the cylinder axis due to the Vϕ velocity component and the eccentricity of the valve (post-valve swirl)

Hr : angular momentum w.r.t. the cylinder axis due to the Vr velocity component and the eccentricity of the valve (post-valve swirl due to the directional effect of the port)

RESULTS

Flow profiles

Figure 3 shows one of the circumferential distributions of radial $\overline{Vr}$, tangential $\overline{V\phi}$, axial $\overline{Vz}$ time mean velocity components and their composite velocities $U=\sqrt{\overline{V\phi}^2+\overline{Vr}^2+\overline{Vz}^2}$ at the distance X of 5mm at the higher lift of 10mm. In the diagram the root mean square (r.m.s.) values of the velocity fluctuatings are also shown. The valve exit flow has two peak velocities around ϕ of 45deg. and -70deg.. $\overline{V\phi}$, which contributes to the pre-valve swirl component, increases remarkably in the azimuthal range of ϕ>60deg.. The axial component Vz increases around ϕ=0deg. which is the location nearest to the cylinder axis.

Horizontal components of the velocities i.e. composites of radial and tangential components $V=\sqrt{\overline{V\phi}^2+\overline{Vr}^2}$ are indicated with the arrows in Fig.4 in which the velocities are normalized by the mean cylinder column speed of induced air. In the azimuthal ranges of
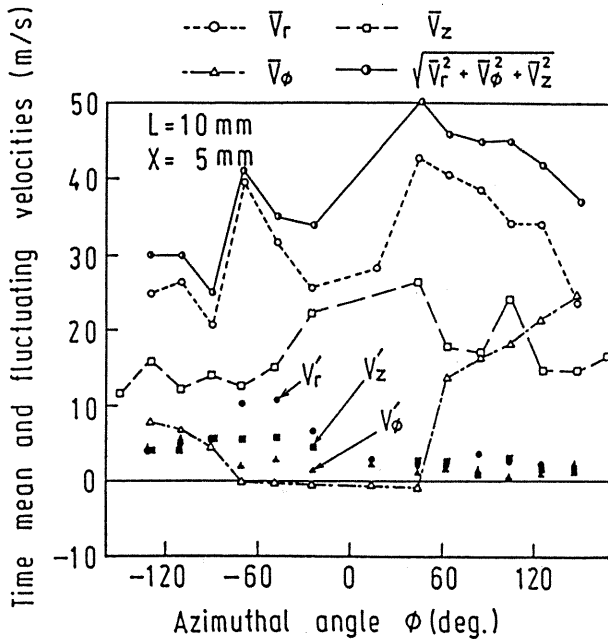

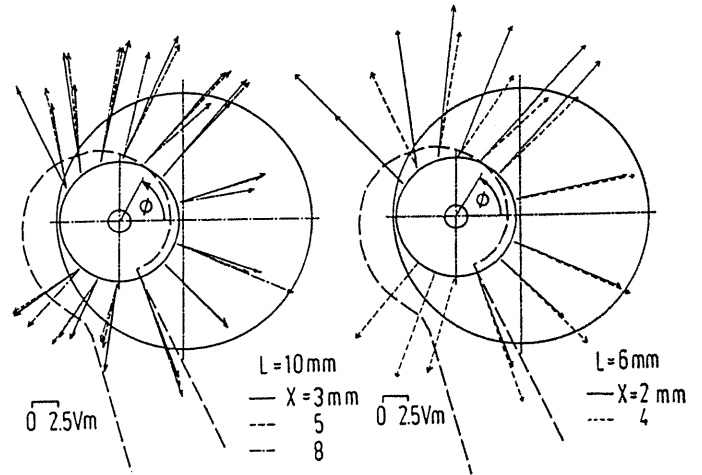
Fig.4 Circumferential distributions of horizontal components of velocities at various distances from cylinder head

ϕ>70deg. and ϕ<-90deg. at both valve lifts and ϕ>70deg. at the lower lift, the more tangential components contributing to swirl generation can be seen. Except for above ranges of ϕ, the velocities are all for the radial direction. With the distance from the cylinder head X increasing, the flow has a trend of inclining into the swirl direction, and which fact implies the flow twists between the top and bottom of the valve gap. The velocities are revealed lower at X=8mm of the higher lift and X=4mm of the lower lift because of the flow with recirculation regions at edges of the valve head.

Figure 5 shows the circumferential distribution of downward inclining angle of valve exit flow δ which is determined by $\tan^{-1}$ $(\overline{Vz}/\overline{V})$. The curved line in the diagram indicates the mean values of δ at the distances from the cylinder head X=3 and 5mm, and δ seems to change symmetrically to the location of ϕ=0deg. at which the flow has a strong downward direction around δ of 50deg.. This strong downward inclining flow directed cylider-diametrically would be supposed to generate the tumbling vortex although the swirl producing capacity is quite small as shown later in Fig.7. In the valve circum-
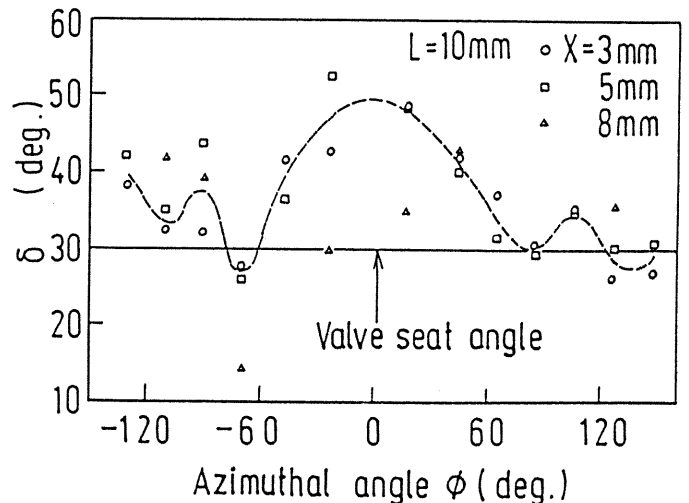

Fig.3 Circumferential distributions of radial Vr, tangential Vϕ and axial Vz time mean velocity components and their fluctuation

Fig.5 Circumferential distributions of downward inclining angle of velocities

ferential range of $\Phi>80$deg. where a strong swirl generation is expected, the flow directs almost parallel to the valve seat angle of 30deg. At the distance X of 8mm, δ changes more widely, which situation would be owing to instability of the flow in the recirculation region of the valve head, described above.

Flow fluctuation

Figure 6 shows the results of statistical analyses of the flow i.e. fluctuating velocity intensity $u'/\bar{U}$, fluctuating flow angle α', and the cross correlations $Cr\Phi$ and $Cv\alpha$. The former correlation is between the instantaneous velocity components of Vr and VΦ and the latter one is between the horizontal velocity component $V=\sqrt{Vr^2+V\Phi^2}$ which is the instantaneous value and its direction given by the angle $\alpha=\tan^{-1}(V\Phi/Vr)$. $\bar{U}$ is the composite of $\bar{V\Phi}$, $\bar{Vr}$ and $\bar{Vz}$ and u' is the composite of fluctuating velocity components of $V\Phi'$, Vr' and Vz' that is $\sqrt{V\Phi'^2+Vr'^2+Vz'^2}$ in which the notations of top bar and prime indicates, respectively, the ensemble averaged velocities and the r.m.s. of fluctuating components. These analyses, except for $u'/\bar{U}$, are based on the instantaneous velocities VΦ and Vr obtained at precisely the same instant by means of the coincidence unit and one thousand pairs of data were sampled at each location. $Cr\Phi$ and $Cv\alpha$ are given by the following equations.

$$Cr\Phi = \frac{\dfrac{1}{n}\sum_{i=1}^{n}(Vri-\bar{Vr})(V\Phi i-\bar{V\Phi})}{\sqrt{\dfrac{1}{n}\sum_{i=1}^{n}(Vri-\bar{Vr})^2}\sqrt{\dfrac{1}{n}\sum_{i=1}^{n}(V\Phi i-\bar{V\Phi})^2}} \qquad (4)$$

$$Cv\alpha = \frac{\dfrac{1}{n}\sum_{i=1}^{n}(Vi-\bar{V})(\alpha i-\bar{\alpha})}{\sqrt{\dfrac{1}{n}\sum_{i=1}^{n}(Vi-\bar{V})^2}\sqrt{\dfrac{1}{n}\sum_{i=1}^{n}(\alpha i-\bar{\alpha})^2}} \qquad (5)$$
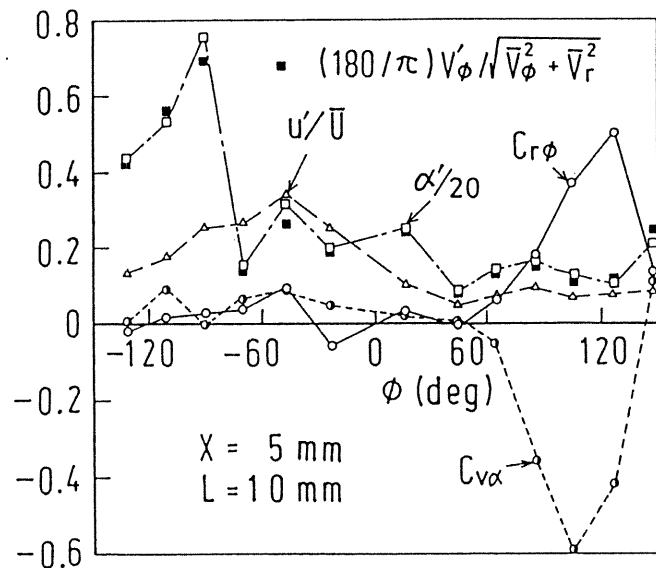

Fig.6 Circumferential distributions of fluctuations of velocity and its direction, and cross-correlations $Cr\Phi$ between Vr and VΦ and $Cv\alpha$ between horizontal velocity and its direction

where n is data sample number.
At X=5mm of the higher valve lift, $u'/\bar{U}$ and α' are lower in $\Phi>30$deg. which corresponds to the downstream side of the valve circumference. In $\Phi<30$deg., however, both fluctuations become higher and $u'/\bar{U}$ takes the maximum at Φ of -45deg., while α' takes the maximum at -90 deg., and thereby the circumferential locations of most highly fluctuating velocity and direction could be seen to differ from each other. Although without displaying diagrams here, these trends were nearly the same as those at the shorter distance from the cylinder head X of 3mm, but at the longer distance of 8mm both fluctuations were higher on the whole of valve circumference.

The solid circles in the diagram indicate the values of $180(V\Phi'/\sqrt{\bar{Vr^2}+\bar{V\Phi^2}})/\pi$ that is the estimation of flow angle fluctuation based on time mean velocity components and these values are almost the same as α' that is the r.m.s. values of α determined by the simultaneous measurements of Vr and VΦ. As a result the fluctuating intensity of the flow direction would be well estimated from separate measurement of velocity components.

The cross correlation profiles in the diagram show that there are the highly positive correlation of $Cr\Phi$ and the highly negative correlation of $Cv\alpha$ around Φ of 120 deg.. The positive correlation means the increment or decrement of VΦ accompanied with Vr. The negative correlation, on the contrary, means the reverse change of V against the flow angle of α. This fact results from the following matter; when both velocity components of Vr and VΦ simultaneously increase or decrease by Vr' and VΦ' from the time mean values, respectively, the flow angle α changes from $\tan^{-1}[(\bar{V\Phi}+V\Phi')/(\bar{Vr}+Vr')]$ to $\tan^{-1}[(\bar{V\Phi}-V\Phi')/(\bar{Vr}-Vr')]$, and the former value of α is less than the latter α when $\bar{V\Phi}$ is comparable with $\bar{Vr}$ and Vr' is higher than VΦ' as Fig.3 shows. These higher correlation suggest a systematic change of the valve flow, and thereby providing the similar existence of such a higher correlation in an operating condition of engine, a cyclic variation of swirl intensity would be suspected to occur because of the flow through this range of Φ having a decisive influence on the swirl generation.
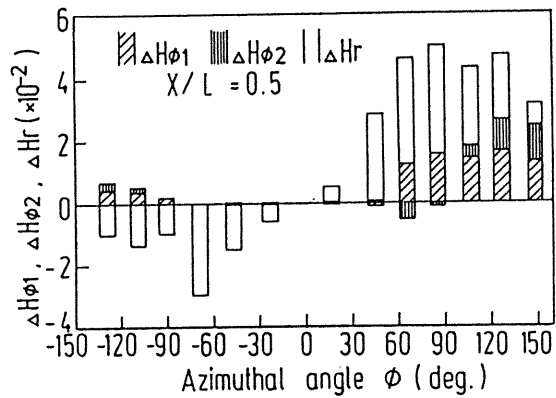
Angular momentum components as swirl generating capacity

The various components of the inlet angular momentum have been calculated based on the time mean velocity data and their circumferential distributions are presented in Fig.7 at the higher valve lift. The vertical axis indicates the angular momentum flow per unit valve curtain area of $\Delta X \Delta \Phi$ Rv where ΔX=1mm and $\Delta \Phi$=10deg. and normalized by $\rho Vm^2\pi Rc^3$ that is air column flow momentum by cylinder radius. The negative value refers to the reverse moment of swirl. The cross-hatched section of the graph is of the pre-valve swirl component $H\Phi 1$ due to $\bar{V\Phi}$, the vertical-striped section of the post-valve swirl component $H\Phi 2$ due to $\bar{V\Phi}$ and the open section of the post-valve swirl component Hr due to $\bar{Vr}$. For both valve lifts, the positive angular momentums are obtained in the positive range of Φ but the reverse momentums are dominant in the negative range, and the positive one reaches the maximum around Φ of 90deg. and the negative one around 70deg.. The angular momentum Hr due to the radial velocity component takes more dominant part of the swirl generation in the pres-
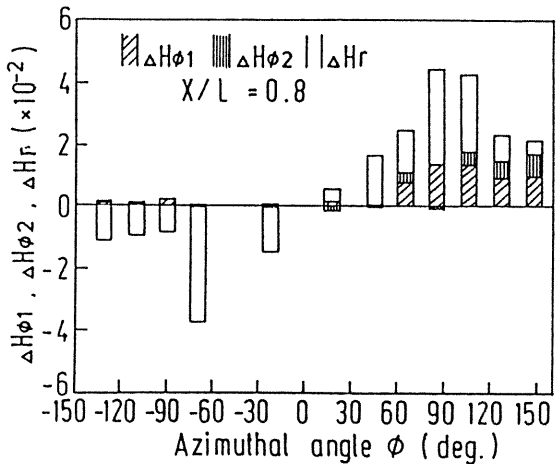
ent port and changes dynamically along the valve circumference. In the forward range of $\Phi > 0$deg., $H\phi 1$ is nearly constant and $H\phi 2$ increases as the measurement point coming to the cylinder wall but they are smaller than Hr. These trends were similar to the lower lift, but Hr, in particular, was more dominant than the higher lift.
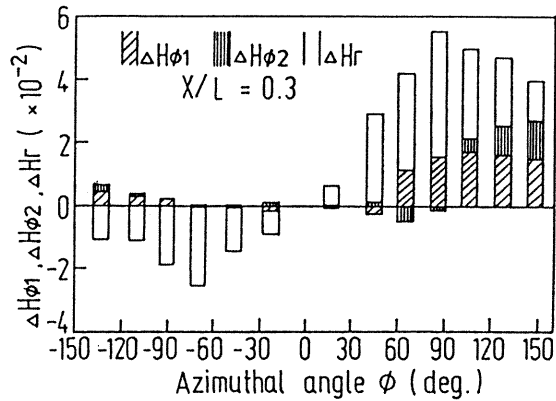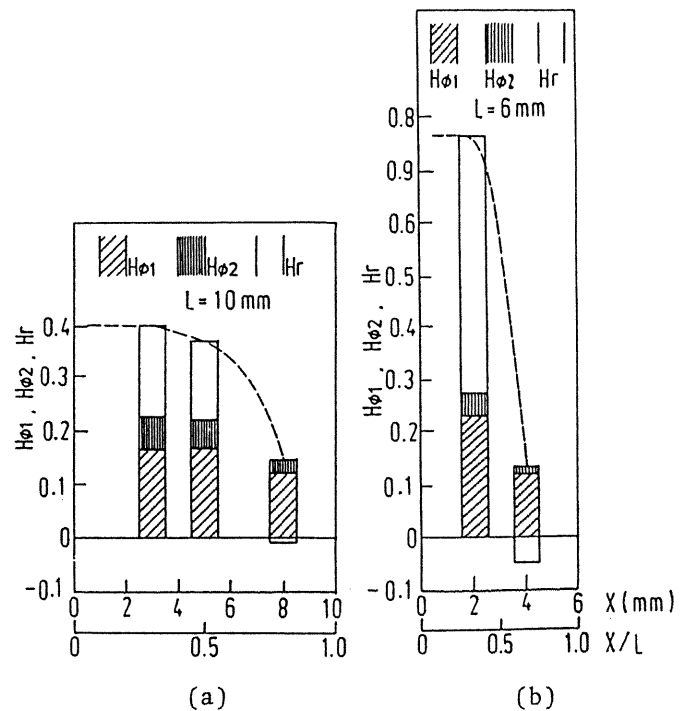
By integrating above angular momentum profiles from -150 to 150deg. of Φ per unit height of the valve curtain area, three components of the angular momentums at various distances of X are shown in Fig.8. The diagram (a) which is the results of the higher valve lift shows $H\phi 1$ nearly constant throughout the valve gap and no vivid change in Hr and $H\phi 2$ at X/L < 0.6, but at X/L=0.8 it shows smaller $H\phi 2$ and negligible Hr. The diagram (b), the results of the lower lift, indicates Hr more predominant than at the higher lift. These results show the trend similar to those reported in Ref.(1), but differ from pre-reported helical port characteristics(10) which indicate that $H\phi 1$ plays predominant role in generating swirl at lower valve lifts and Hr becomes important at higher lifts. In both diagrams of Fig.8, the values of the angular momentum flux at the lowest locations exceeding about 70% of the valve lifts are small comparing with other locations, which fact suggests no significant contribution to the total angular momentum because of these locations being inside the recirculation regions at edges of valve head.

The total swirl producing capacity of the port has been estimated by integrating the angular momentum per unit length of lift over the whole valve gap. Due to the limited number of velocity locations, data were interpolated and extrapolated in the portion of lack of data as indicated by the broken line in the diagrams. The integration results are 2.33 and 1.99 which correspond to swirl ratios (solid body rotational speed of swirl/engine speed) of 3.26 and 2.79 at the valve lift of 10 and 6mm, respectively, where the engine speeds are based on the mean piston speeds equal to the cylinder column speeds of induced air in the steady flow test, and accordingly the swirl producing capacity becomes higher at the higher valve lift.

(a)

(b)

(c)

Fig.7 Circumferential distributions of normalized inlet angular momentum components $\Delta H\phi 1, \Delta H\phi 2, \Delta Hr$

Fig.8 Contributions of angular momentum components to swirl

CONCLUSIONS

By measuring three time-mean velocity components and two instantaneous components at the inlet valve curtain area under steady flow condition by means of the two dimension LDA system comprising the coincident data acquisition unit, the helical port of DI diesel engine revealed the following valve flow characteristics;

1. Two cross-correlations, one is between the radial and tangential velocity components and the other is between their composite velocity and its direction become higher in the vicinity of the cylinder wall on the downstream side of the valve periphery, though the latter cross-correlation being negative. These higher correlations suggest a systematic change of valve flow which would relate with cyclic variation of swirl in an operating condition of engine.

2. The flow velocity and its direction fluctuate stronger from time to time in backward side of the valve periphery than forward side.

3. The flow angle inclining from the cylinder head surface become larger than the valve seat angle in the neighborhood of the cylinder axis and changes symmetrically to the location nearest to the cylinder axis.

4. The directional swirl component of the total angular momentum which is attributed mainly to port orientation plays the dominant role and its contribution increases with an increase of the valve lift.

5. The pre-valve swirl component of the total angular momentum which is attributed to the helical geometry of the port appears on the downstream side of the valve periphery mainly and its role becomes recessive at the lower valve lift.

REFERENCES

1. Kajiyama, K., Nishida, K., Murakami, A., Arai, M. and Hiroyasu, H., "An Analysis of Swirling Flow in Cylinder for Predicting DI Diesel Engine Performances," SAE Paper 840518, 1984.
2. Begleris, P. and Gosman, A. D., "Analysis of In-Cylinder Flow Generation by Helical Ports," Proc. Symp. on Fluid Flow and Heat Transfer in Reciprocating Machinery," ASME Winter Meeting, 1987.
3. Uzkan, T., Borgnakke, C. and Morel, T., "Characterization of Flow Produced by a High-Swirl Inlet Port," SAE Paper 830266, 1983.
4. Tindal, M. J., Williams, T. J. and Aldoory, M., "The Effect of Inlet Port Design on Cylinder Gas Motion in Direct Injection Diesel Engines," Proc. Symp. on Flows in IC Engines, ASME Winter Annual Meeting, Phoenix, 1982.
5. Arcoumanis, C. and Whitelaw, J. H., "Are Steady Flow Inlet Boundary Conditions Valid for Engine Cylinder Calculations?," Proc. Cong. on Modeling of IC Engines, Valencia, 1987.
6. EI Tahry, S. H., Khalighi, B. and Kuziak, Jr. W. R. "Unsteady Flow Velocity Measurements around an Intake Valve of a Reciprocating Engines," SAE Paper 870593, 1987.
7. Khalighi, B., EI Tahry, S. H. and Kuziak, W. R., "Measured Steady Flow Velocity Distributions around a Valve/Seat Annulas," SAE Paper 860462, 1986.
8. Gosman, A. D., "Multidimensional Modelling of Cold Flows and Turbulence in Reciprocating Engines," SAE Paper 850344, 1985.
9. Wakisaka, T., Shimamoto, Y. and Isshiki, Y., "Three-Dimensional Numerical Analysis of In-Cylinder Flows in Reciprocating Engines," SAE Paper 860464, 1986.
10. Arcoumanis, C. and Tanabe, S., "Swirl Generation by Helical Ports," SAE Paper 890790, 1989.